HHS Public Access

Author manuscript

Bone. Author manuscript; available in PMC 2020 October 01.

Published in final edited form as:

Bone. 2019 October ; 127: 376–385. doi:10.1016/j.bone.2019.07.009.

Cbl-PI3K Interaction Regulates Cathepsin K Secretion in Osteoclasts

Jungeun Yu, **Naga Suresh Adapala**, **Laura Doherty**, **Archana Sanjay**[#]

Department of Orthopaedic Surgery, UConn Health, Farmington, CT 06030

Abstract

Effective bone resorption by osteoclasts is critical for balanced bone remodeling. We have previously reported that mice harboring a substitution mutation of tyrosine 737 to phenylalanine in the adapter protein Cbl (Cbl^{Y737F}, YF) have increased bone volume partly due to decreased osteoclast-mediated bone resorption. The Cbl^{Y737F} mutation abrogates interaction between Cbl and the p85 subunit of PI3K. Here, we studied the mechanism for defective resorptive function of YF mutant osteoclasts. The YF osteoclasts had intact actin cytoskeletons and sealing zones. Expression and localization of proteins needed for acidification of the resorptive lacunae were also comparable between the WT and YF osteoclasts. In contrast, secretion of Cathepsin K, a major protease needed to degrade collagen, was diminished in the conditioned media derived from YF osteoclasts. The targeting of Cathepsin K into LAMP2-positive vesicles was also compromised due to decreased number of LAMP2-positive vesicles in YF osteoclasts. Further, we found that in contrast to WT, conditioned media derived from YF osteoclasts promoted increased numbers of alkaline phosphatase (ALP)-positive colonies, and increased expression of osteogenic markers in WT calvarial cultures. Cumulatively, our results suggest that the Cbl-PI3K interaction regulates Cathepsin K secretion required for proper bone resorption, and secretion of factors which promote osteogenesis.

Keywords

Osteoclast; vesicular trafficking; Cathepsin K; LAMP2; PI3K and Cbl

Introduction

Osteoclasts are large, multinucleated cells with a unique capacity to degrade the organic and inorganic bone matrices. This function is absolutely necessary for bone modeling bone remodeling and to maintain calcium and phosphate ion homeostasis [1] . The resorptive

[#]**Corresponding Author:** Archana Sanjay, Department of Orthopaedic Surgery, UConn Health, 263 Farmington Ave, Farmington, CT, 06030. Tel: 860-679-4649; asanjay@uchc.edu.

Author Contributions: J.Y., N.S.A. and L.D. performed experiments, and analyzed the data. A.S. designed the study, analyzed data, and wrote the manuscript. All authors have reviewed and approved the final submission.

Disclosure: The authors have nothing to disclose.

function of osteoclasts also plays a role in the formation of hematopoietic stem cell niches in the bone marrow [2, 3]. Because osteoclasts are a fundamental factor in the pathogenesis of virtually all diseases associated with bone loss, the insights gained into the mechanisms by which they form and degrade bone are clinically significant.

Phosphatidylinositol-3 Kinase (PI3K) is a prominent lipid kinase that phosphorylates the 3'-hydroxyl group on the inositol ring of phosphatidylinositol. PI3K is stimulated by Macrophage colony stimulating factor (M-CSF) and $\alpha_v\beta_3$ integrins, both of which are critical for osteoclast resorptive function. Based on the sequence similarity, composition of subunits and substrate specificity, PI3Ks are divided into three classes: Class I, II, and III. While class II and III PI3Ks are constitutively activated, Class I PI3Ks are activated in response to extracellular stimuli. Class I PI3K is a heterodimer of p110 catalytic and p85 regulatory subunits. The p110 catalytic subunit binds to the p85 regulatory subunit with high affinity and this interaction prevents inadvertent activation of PI3K [4, 5]. Upon engagement of the SH2 domain of the p85 subunit through binding to phosphorylated tyrosines of receptors or signaling proteins, the inhibitory effect of p85 on p110 is released, resulting in increased lipid kinase activity [6].

The E3 ubiquitin ligase Cbl is an adaptor protein that regulates PI3K signaling via interaction with the p85 regulatory subunit [7]. In macrophages, Src family kinase-mediated phosphorylation of Cbl is required for Cbl-PI3K association, and for the transfer of this complex to the actin rich cytoskeleton [8]. In the skeletal system, Cbl plays an important role in bone remodeling by regulating bone resorption of osteoclasts [9–11]. While establishing a role for Cbl in bone resorption [9, 12, 13], we identified a unique function of Cbl through the requirement of a tyrosine at 737 in the C-terminal half, for its interaction with the SH2 domain of the p85 regulatory subunit of PI3K [14]. Substitution mutation of the tyrosine 737 into phenylalanine ($Cb1_{Y737F}$) resulted in abrogation of Cbl-p85 association, [15] but did not impact the E3 ligase activity of Cbl and the protein level of p85 [16]. We have shown that Src-mediated phosphorylation of Cbl is required for Cbl-p85 interaction, and adenoviral overexpression of $Cb1^{Y737F}$ in WT osteoclasts decreased pit forming activity [10, 11, 15].

To study the impact of the Cbl-PI3K interaction in the skeletal system, a global knock-in mouse model in which the tyrosine 737 was substituted to phenylalanine ($Cbl^{Y737F/Y737F}$ mice; hence forth YF mice) was used [17]. Our skeletal characterization of YF mice demonstrated that both bone resorption and formation are perturbed. Increased bone volume resulted due to defective osteoclast-mediated resorption both during homeostasis and upon acute estrogen deprivation [16, 18]. In this study, we investigated the molecular mechanism that leads to decreased osteoclast function in YF mice.

Materials and Methods

Mice

Generation of $Cbl^{Y737F/Y737F}$ (YF) mice with a point mutation on the p85 regulatory subunitbinding site of Cbl were previously described [17]. Mice were genotyped for WT and YF alleles as previously reported [16]. All mice used in the study were in a mixed C57BL/6JX129SvJ background. For all experiments, 6-8 week old mice were used. All animal

procedures were conducted according to protocols approved by the University of Connecticut Health Center Animal Care Committee. Experiments were repeated at least three times, and each time a different cohort of WT and YF mice were used to generate primary osteoclast cultures.

Culture of bom marrow-derived macrophages and osteoclast formation

To obtain BMMs, marrow was removed by flushing with a 26-gauge needle and erythrocytes were lysed in 150 mM NH_4Cl, 10 mM $KHCO_3$, and 0.1 mM EDTA (pH 7.4). Cells were centrifuged and the pellet was suspended in Minimum essential mediumα-modification (αMEM) in the presence of 10% fetal bovine serum (FBS) (both from Sigma-Aldrich, St. Louis, MO). Cells were seeded at a density of 300,000 cells/cm^2 and cultured for 3 to 4 days on petri dishes in the presence of recombinant human M-CSF at 30 ng/ml. M-CSF cDNA and expression vectors were obtained from Dr. D. Fremont (St. Louis, MO) and M-CSF purified as previously reported [19]. For osteoclast formation, cells were collected following treatment with 0.25% trypsin/EDTA for 5 min and seeded at a density of 47,000 cells/cm^2 in αMEM with 10% FBS, M-CSF at 30 ng/ml, and recombinant murine RANKL at 10 ng/ml. RANKL cDNA and expression vectors were obtained from Dr. M. Glogauer (Toronto, Canada), and GST-tagged RANKL was expressed and purified as described [20]. Cultures were carried out until formation of multinucleated TRAP-positive cells. TRAP enzyme histochemistry was conducted using a commercial kit (Sigma-Aldrich, St. Louis, MO), in accordance with manufacturer's instructions. TRAP-positive cells containing more than 3 nuclei were considered osteoclasts. To produce conditioned media, BMMs were either cultured in αMEM with M-CSF (20 ng/ml) for 5 days on petri dishes. To generate osteoclast-conditioned medium, BMMs were cultured on HA-coated plates in the presence of M-CSF (20 ng/ml) and RANKL (50 ng/ml) for 6 days. Conditioned media was harvested and centrifuged at 100,000g for 1 h at 4 °C. The supernatant was filtered through 20-micron filters and either immediately used or stored at −80 °C. CD1 calvarial osteoprogenitors were derived from 2-5 day old CD-1 pups as described previously [16]. After seven days, cultures were stained for toluidine blue and ALP staining as per manufacturer's instructions or harvested to isolate mRNA.

Quantitative reverse transcription PCR

To analyze expression of differentiation markers by real time PCR, cells were lysed with Trizol (Thermo Fisher Scientific, Waltham, MA), and RNAs were extracted as per manufacturer's instructions, 1μg of RNA was treated with DNase (Thermo Fisher Scientific), and reverse transcribed to cDNA using the Superscript III cDNA Synthesis Kit (Thermo Fisher Scientific). Quantitative reverse transcription-PCR (qRT-PCR) was performed with 10ng of cDNA per reaction using SYBR Green Master Mix (Thermo Fisher Scientific) and validated custom designed primers. All primers used in the study are listed in Table 1. ABI Step One Plus Real Time PCR System using the following thermal cycler program: 95° C for 10 minutes, 40 cycles of 95° C for 15 seconds, and 57° C for 1 minute. Product specificity was confirmed by melt curve analysis, and relative expression was determined using ΔΔCT analysis after normalization to *Gapdh* expression.

Bone resorption

In vitro bone resorbing activity was assayed as described previously [12, 16]. Briefly, osteoclasts were generated in Collagen gel (Nitta Gelatin Co., Osaka, Japan). After 6 days of culture, mature osteoclasts were released from Collagen gel by gentle digestion with 0.1% Collagenase (Calbiochem, San Diego, CA), and cells were seeded onto sterile bovine bone discs in 96-well plates. 48 hours later, bone discs were immersed in 1 M Ammonium hydroxide (Sigma-Aldrich) for 5 min, sonicated for 10 s, and then stained for 4 min with 1% toluidine blue in 1% sodium borate (both from Sigma-Aldrich) and briefly rinsed in water. Pit area was quantified with the measuring tool in Adobe Photoshop CS3 Extended Edition, and was normalized to the number of osteoclasts actually present in each sample, determined by counting osteoclasts that were plated on tissue culture plastic.

Inorganic matrix resorption

Mature osteoclasts developed on collagen gel as described above. Cells (10^5) were then seeded onto HA-coated wells (BD BioCoat™ Osteologic™, BD Bioscience, San Jose, CA). One day after, wells were rinsed in water and treated with 5% sodium hypochlorite for 5 minutes. Analysis of resorbed area was performed using bright field microscopy.

Fluorescence Microscopy

Cells were plated on sterile FBS-coated glass coverslips (Corning Inc. Corning, NY) and fixed in PBS containing 4% paraformaldehyde for 10 min, then permeabilized with 0.3% Triton X-100 (all from Sigma-Aldrich) for 5 min. Coverslips for Actin labeling were incubated in a 1:40 dilution in PBS of rhodamine-phalloidin stock solution (Thermo Fisher Scientific) for 20 min. To detect presences of enzymes, cells were incubated overnight at 4 °C with primary antibodies diluted in PBS supplemented with 3% bovine serum albumin (BSA, Sigma-Aldrich). Cells were rinsed with PBS and then incubated with secondary antibodies conjugated to fluorescein isothiocynate (FITC) or Phycoerythrin (PE) (both from Thermo Fisher Scientific) for 1 h at room temperature. The following antibodies were used: anti-vATPase (E subunit) antibody (gift from Dr. Bet Lee, Ohio State University), anti-LAMP2, anti-Cathepsin K, and anti-Cathepsin D (Santa Cruz Biotechnology, Dallas, TX). To visualize nuclei, cells were stained with DAPI (Thermo Fisher Scientific) before mounting. Cells were examined on a Leica fluorescence microscope (Model DMI6000B), and images were collected using the Leica Application Suite X CLAS X 1.5.1.1387 (Leica Microsystem, Buffalo Grove, IL). For labeling lysosomes in live cells, cells were stained with LysoTracker® fluorescent dye (Thermo Fisher Scientific) as per manufacturer's instructions. LAMP2 positive vesicles were quantified by using counting tool from LASX after imaging and the number was normalized by number of nuclei stained with DAPI.

Cathepsin K and Cathepsin D secretion

Mature osteoclasts were seeded onto 24-well plates (50,000 cells/well). Cells were cultured in the presence of 10% FBS containing medium for 24 h. Conditioned media was collected, and cells were harvested and lysed in mRIPA buffer for SDS-PAGE analysis to detect the presence of proteins.

Western blotting analysis

Clarified total cell lysate was electrophoresed on 10 or 12% SDS-PAGE as previously described [18]. Western blots were probed with anti-Cathepsin K or anti-Cathepsin D antibodies; the blots were stripped and reprobed with anti-β-Actin antibodies (Cell Signaling Technology, Danvers, MA). The amount of protein in individual bands was quantified by using Odyssey Infrared Imaging Systems software 2.1 (LI-COR Biosciences, Lincoln, NE) as previously reported [16, 21].

Statistical Analysis

Experiments conducted in this study were repeated at least three times. Data were expressed, as the mean ± SD. Significant differences were determined using Student′s *t*-test, $p < 0.05$ vs. control was considered significant.

Results

Actin organization and sealing zone formation are intact but bone resorption is decreased in YF osteoclasts

To resorb bone, mature osteoclasts attach to bone via integrin-regulated rearrangement of the cytoskeleton, creating a sealing zone that is necessary for activation and polarization of osteoclasts. Osteoclasts were seeded on glass or bovine bone discs, and were stained with rhodamine-phalloidin to visualize actin cytoskeleton organization. Both WT and YF osteoclasts formed the typical actin ring on glass cover slips and sealing zone on bone discs, suggesting that the Cbl-PI3K interaction is not required for organization of actin cytoskeleton or the sealing zone formation (Fig. 1A and B). We also determined the *in vitro* pit forming activity of osteoclasts plated on bovine bone discs. In agreement with our previously published results [12, 16] we found that compared to WT osteoclastss, YF osteoclastss formed shallower pits, and there was a 60% decrease in resorbed area pit area (Fig. 1C and D) as we have reported previously[16, 21].

Expression of factors needed for acid formation is not altered in YF osteoclasts

Following sealing zone formation, the ruffled border is generated by the simultaneous fusion of numerous secretory lysosomes with the plasma membrane [22]. The ruffled border functions as a site of secretion and externalization of hydrochloric acid and proteases. The acidic environment of osteoclasts dissolves hydroxyapatite (HA), and the proteases hydrolyze the collagen-rich organic matrix [23]. To examine acid secretion, WT and YF osteoclasts were plated on HA-coated surfaces (Fig. 2A). The resorbed area was about 20% decreased in YF osteoclastss, but was not statistically different from WT (Fig. 2B). Proteins implicated in acidification of resorption lacuna include carbonic anhydrase, chloride channel, and vacuolar ATPase. Consistent with no significant difference in resorption of HA-coated slides, which occurs exclusively through release of protons and acidification of the resorptive lacune, immunofluorescence analysis showed that the cellular localization of vATPase [24] was also comparable between the two genotypes (Fig. 2C) . We found that expression of mRNA for *Car2, Clc7,* and *Atp6v0d2* was comparable between WT and YF osteoclasts (Fig.2D). Together these results suggest that the loss of the Cbl-PI3K interaction

in osteoclasts attenuates bone resorption, but does not regulate components of the acid-generating machinery.

The number of LAMP2-positive vesicles is significantly decreased in YF osteoclasts

Bone resorption by osteoclasts is highly dependent on lysosomes that release proteases in the resorption lacuna. We observed lysosomes in osteoclasts using LysoTracker fluorescent dye. We found that LysoTracker staining was attenuated in YF osteoclasts compared to WT (Fig. 3A). Osteoclasts were also stained for LAMP2, an integral lysosomal membrane protein [25]. We found that the number of LAMP2-positive vesicles in each osteoclast was significantly decreased in YF osteoclasts compared to WT (Fig. 3B and C). In order to understand the reason for decreased LAMP2 positive lysosomes in YF osteoclasts, we determined expression of the MITF/TFE family of transcription factors that is required for lysosomal biogenesis[6]. We found that the expression of *Mtif, TfeB,* and *Tfe3* was comparable between WT and YF osteoclasts (Supplementary Figure 1). Together, these results suggest that the loss of Cbl-p85 interaction in osteoclasts results in decreased numbers of LAMP2-positive lysosomes, but this interaction is not involved in regulating the transcription factors needed for lysosomal biogenesis.

Secretion of Cathepsin K is decreased in YF osteoclasts

Lysosomal proteases required for bone resorption include Tartrate acid resistant phosphatase (TRAP) and Cathepsin K [1]. Most proteases, including Cathepsin D, K, and TRAP are synthesized in the rough endoplasmic reticulum (rER) as a pro-form, and later cleaved into a mature form in the lysosomes [27, 28]. The mRNA levels of *Acp5* and *Ctsk* were significantly increased in YF osteoclasts (Fig. 4A). After synthesis in the endoplasmic reticulum, these enzymes are transported from trans Golgi network (TGN) to the secretory lysosomes (SL), which have all the features of lysosomes, but undergo regulated secretion in response to specific stimuli [29]. While a substantial amount of TRAP is secreted directly from TGN, the majority of Cathepsin K is found in SL [30]. We examined the protein expression and secretion of Cathepsin K. For these experiments, equal numbers of mature osteoclasts were plated (Fig. 4B). We found that compared to WT, there was about a 2-fold increase in Cathepsin K protein level in total cell lysates, but the amount of Cathepsin K secreted by YF osteoclasts in the conditioned media was significantly diminished (~75% decrease) (Fig. 4C, left, and 4D). In contrast, protein expression and secretion of Cathepsin D, an aspartic protease mostly present in lysosomes [31], was comparable between WT and YF osteoclasts (Fig. 4C, right). Next we examined the cellular distribution of Cathepsin K. Mature osteoclasts grown on bone slices were stained with rhodamine phalloidin to visualize actin cytoskeleton. As reported by others we also found that in WT osteoclasts, Cathepsin K exclusively localized within actin ring. In contrast, in a majority of YF osteoclasts, Cathepsin K distribution was not within the actin ring (Supplementary Figure 2A and B). Further, compared to WT, colocalization of Cathepsin K within LAMP2-positive vesicles was also decreased in YF osteoclasts (Supplementary Figure 2C).

Conditioned media derived from YF osteoclasts enhances osteogenesis

Independent of their resorptive activity, osteoclasts also regulate bone formation [24, 32]. YF mice also have increased numbers of dysfunctional osteoclasts and an increased bone

formation rate [16, 33]. Therefore, we investigated whether YF osteoclasts can also induce osteogenesis *in vitro.* To test this, bone marrow-derived sorted $CD11b^+$ cells were cultured in the presence of M-CSF to generate BMMs, or were seeded onto HA-coated surfaces with M-CSF and RANKL to obtain osteoclasts. Conditioned media from BMMs and mature osteoclast cultures was harvested. WT calvarial osteoblasts were grown in the presence of conditioned media derived from BMMs or osteoclasts of WT or YF mice, and then stained for the formation of CFUs and ALP-stained colonies. We found that cells treated with the YF osteoclast conditioned media had more CFUs and ALP-positive colonies, and expressed increased osteogenic markers than those treated with WT osteoclast conditioned media or either WT or YF BMM conditioned media (Figure 5 and data not shown for BMM conditioned medium). In osteoclasts derived from $Ctsk^{-/-}$ mice, mRNA expression of sphingosine kinase (SphK1) is upregulated [34]. SphK1 catalyzes the formation of sphingosine-1-phosphate (S1P), and S1P secreted by osteoclasts promotes osteogenesis [34, 35]. To determine osteogenic factors generated by osteoclasts, cells were cultured on HA-coated plates and harvested for qRT-PCR analysis. We found that RNA expression for Wnt10B, BMP6, PDGF-BB, and Sphk1 and 2 were comparable between WT and YF cells (Table 2).

Discussion

In osteoclasts, levels of Cathepsin K far exceed that of other proteases [36–38]. It is unique among the mammalian proteases in its ability to cleave both telopeptides and helical region of collagen type I [39]. In humans, mutations in *CTSK* cause pycnodysostosis [37, 40]. In $Ctsk^{-/-}$ mice, osteoclasts differentiate normally, but degrade the collagenous matrix poorly [39, 41]. However, the signaling pathways that regulate Cathepsin K secretion are not completely understood.

In this report, we have demonstrated that abrogation of the Cbl-PI3K interaction in osteoclasts results in decreased lysosome numbers and mis-localization of Cathepsin K, contributing to decreased Cathepsin K secretion, thereby resulting in decreased pit formation. Towards this, our previous work shows increased bone volume and decreased serum level of carboxyterminal collagen crosslinks (CTX) during homeostasis and upon ovariectomy in YF mice [16, 18].

In osteoclasts, a family of v-ATPases function to acidify lysosomes by coupling ATP hydrolysis to proton transport. To maintain electron neutrality, a parallel transport of chloride ions into the lacuna takes place simultaneously. We found that the localization of v-ATPase was also unperturbed in the absence of Cbl-PI3K interaction. While Cathepsin K and v-ATPase are of lysosomal origin, our results suggest that PI3K signaling is preferentially involved in trafficking and secretion of Cathepsin K. These findings suggest that vesicle cargo may be a determining factor in how secretory vesicles are transported to the plasma membrane for exocytosis.

YF osteoclasts are defective in secreting Cathepsin K, but secretion of Cathepsin D is normal. These data suggest that in YF osteoclasts, the cargo present in the secretory lysosomes is not secreted properly, while other secretory mechanisms are not perturbed. The

Protein kinase C-δ deficiency in osteoclasts does not affect v-ATPase localization, but attenuates Cathepsin K secretion [42]. Differential secretion and targeting of vesicles is supported by other studies. Disruption of the Mannose-6-phosphate pathway in osteoclasts augmented Cathepsin K secretion without affecting Cathepsin D targeting and secretion [30]. Our results and other findings suggest the existence of distinct/different pools of secretory lysosomes in osteoclasts, each relying on specific signaling cues essential for their exocytosis. This flexibility will allow cells to secrete cargo based on need.

AKT, a serine/threonine kinase, is the major effector of PI3K in several cell types, including bone cells. We reported that in YF mice, AKT is constitutively phosphorylated, and there is increased phosphorylation of AKT substrates in osteoclasts [12, 16]. AKT substrates that are postulated to regulate vesicle include the Rab GTPase-activating proteins AS160/TBC1D4 [43] and TBC1D1[44]; AKT binding protein ClipR-59 [45]; and CENTB1/ACAP1 and CENTG1 in the centaurin family of GTPases [46, 47]. We have also reported that activation of small GTPase is perturbed in YF osteoclasts. Given these findings, we speculate that in YF osteoclasts, decreased lysosome numbers and perturbed AKT activation could impact targeting of Cathepsin K to secretory vesicles, and eventually, bone resorption.

In addition to AKT, other Cbl-related pathways could also regulate vesicular trafficking. A subset of autophagy related proteins were reported to regulate lysosomal secretion in osteoclasts [48]. Interestingly, of the autophagy proteins, microtubule associated protein 1 light chain 3 (LC3) directly binds Cbl via a LC3 interacting motif (WxxL) present in the C-terminal end of Cbl [49]. While binding of mutated Cbl and other signaling proteins such as Src and Grb2 was not affected [16], whether disruption in LC3 binding to mutated Cbl protein, and its impact on Cathepsin K secretion, remain to be tested.

Independent of their resorptive activity, osteoclasts also regulate bone formation. This is especially the case in non-resorptive osteoclasts [24, 50]. *Ctsk*$^{-/-}$ mice have increased osteoclast numbers and bone formation rates [37, 41, 51], and *in vitro* data indicate that osteoclast-specific deletion of *Ctsk* stimulates bone formation [34]. Like *Ctsk*$^{-/-}$ mice, global YF mice also exhibit increased numbers of dysfunctional osteoclasts and an increased bone formation rate [12, 16, 33]. Additionally, as demonstrated here, Cathepsin K secretion was perturbed in YF osteoclasts. Therefore, we investigated whether YF osteoclasts can influence osteoblast proliferation and differentiation. Our findings show that conditioned media derived from YF osteoclasts enhances osteogenesis. We found that SphK-1 and 2 expression levels were similar between WT and YF samples. mRNA expression levels of other known factors secreted by osteoclasts that modulate osteogenesis were also comparable between WT and YF osteoclasts [24, 32, 52]. These data suggest that the *Ctsk* $^{-/-}$ osteoclasts and dysfunctional YF osteoclasts secrete different factors that promote osteogenesis. We propose that Cbl-PI3K signaling regulates osteoclast-derived factors that promote osteogenesis, however, experiments to identify the factor(s) are warranted.

The *in vivo* significance of our findings highlights that the selective disruption of Cathepsin K secretion has important implication on bone health. YF mice have increased bone mass under homeostatic conditions [16]. Additionally, YF mice are protected from experimental postmenopausal osteoporosis [18]. Osteoclasts are also responsible for cancer progression

[53] and there is a strong correlation between Cathepsin K expression and metastatic tumors [54, 55]. More than 30 inhibitors of PI3Ks and AKT have been developed for anticancer therapy, and some of them have entered clinical trials [56–58]. Our results suggest that the selective disruption of the Cbl-PI3K interaction can be a strategy to prevent pathological bone loss in several clinical settings, including cancer.

Supplementary Material

Refer to Web version on PubMed Central for supplementary material.

Acknowledgments

The authors thank D. Fremont for M-CSF cDNA and M. Glogauer for *Tnfsf11* cDNA, B. Lee for the anti vATPase (E subunit) antibody. National Institute of Health Grant (AR0550601) to A.S supported part of the work.

References

[1]. Teitelbaum SL. Bone resorption by osteoclasts. Science 2000;289: 1504–1508. [PubMed: 10968780]

[2]. Kollet O, Dar A, Shivtiel S, Kalinkovich A, Lapid K, Sztainberg Y, Tesio M, Samstein RM, Goichberg P, Spiegel A, Elson A, Lapidot T. Osteoclasts degrade endosteal components and promote mobilization of hematopoietic progenitor cells. Nature medicine 2006;12: 657–64.

[3]. Mansour A, Wakkach A, Blin-Wakkach C. Role of osteoclasts in the hematopoietic stem cell niche formation. Cell Cycle 2012;11: 2045–6. [PubMed: 22580466]

[4]. Cantley LC. The phosphoinositide 3-kinase pathway. Science 2002;296: 1655–7. [PubMed: 12040186]

[5]. Engelman JA, Luo J, Cantley LC. The evolution of phosphatidylinositol 3-kinases as regulators of growth and metabolism. Nature reviews. Genetics 2006;7: 606–19.

[6]. Foukas LC, Okkenhaug K. Gene-targeting reveals physiological roles and complex regulation of the phosphoinositide 3-kinases. Archives of biochemistry and biophysics 2003;414: 13–8. [PubMed: 12745249]

[7]. Swaminathan G, Tsygankov AY. The Cbl family proteins: ring leaders in regulation of cell signaling. Journal of cellular physiology 2006;209: 21–43. [PubMed: 16741904]

[8]. Meng F, Lowell CA. A b1 integrin signaling pathway involving Src-family kinases, Cbl and PI-3 kinase is required for macrophage spreading and migration. The EMBO journal 1998;17: 4391–4403. [PubMed: 9687507]

[9]. Chiusaroli R, Sanjay A, Henriksen K, Engsig MT, Horne WC, Gu H, Baron R. Deletion of the gene encoding c-Cbl alters the ability of osteoclasts to migrate, delaying resorption and ossification of cartilage during the development of long bones. Dev Biol 2003;261: 537–47. [PubMed: 14499658]

[10]. Miyazaki T, Sanjay A, Neff L, Tanaka S, Horne WC, Baron R. Src kinase activity is essential for osteoclast function. The Journal of biological chemistry 2004;279: 17660–6. [PubMed: 14739300]

[11]. Sanjay A, Houghton A, Neff L, DiDomenico E, Bardelay C, Antoine E, Levy J, Gailit J, Bowtell D, Horne WC, Baron R. Cbl associates with Pyk2 and Src to regulate Src kinase activity, alpha(v)beta(3) integrin-mediated signaling, cell adhesion, and osteoclast motility. J Cell Biol 2001;152: 181–95. [PubMed: 11149930]

[12]. Adapala NS, Barbe MF, Tsygankov AY, Lorenzo JA, Sanjay A. Loss of Cbl-PI3K interaction enhances osteoclast survival due to p21-Ras mediated PI3K activation independent of Cbl-b. Journal of cellular biochemistry 2014;115: 1277–89. [PubMed: 24470255]

[13]. Nakajima A, Sanjay A, Chiusaroli R, Adapala NS, Neff L, Itzsteink C, Horne WC, Baron R. Loss of Cbl-b increases osteoclast bone-resorbing activity and induces osteopenia. Journal of bone and

mineral research : the official journal of the American Society for Bone and Mineral Research 2009;24: 1162–72.

[14]. Songyang Z, Cantley LC. Recognition and specificity in protein tyrosine kinase-mediated signaling. Trends Biochem. Sci. 1995;20: 470–475. [PubMed: 8578591]

[15]. DeBlasi G, Sanjay A, Miyazaki T, Horne WC, Baron R. c-Cbl,but not Cbl-b,requires Src phosphorylation to interact with hte p85 subunit of PI3kinase. J Bone Miner Res 2002;17 (Suppl. 1): S350.

[16]. Adapala NS, Barbe MF, Langdon WY, Nakamura MC, Tsygankov AY, Sanjay A. The loss of Cbl-phosphatidylinositol 3-kinase interaction perturbs RANKL-mediated signaling, inhibiting bone resorption and promoting osteoclast survival. The Journal of biological chemistry 2010;285: 36745–58. [PubMed: 20851882]

[17]. Molero JC, Turner N, Thien CB, Langdon WY, James DE, Cooney GJ. Genetic ablation of the c-Cbl ubiquitin ligase domain results in increased energy expenditure and improved insulin action. Diabetes 2006;55: 3411–7. [PubMed: 17130487]

[18]. Adapala NS, Holland D, Scanlon V, Barbe MF, Langdon WY, Tsygankov AY, Lorenzo JA, SanJay A. Loss of Cbl-PI3K interaction in mice prevents significant bone loss following ovariectomy. Bone 2014;67C: 1–9.

[19]. Lee SH, Rho J, Jeong D, Sul JY, Kim T, Kim N, Kang JS, Miyamoto T, Suda T, Lee SK, Pignolo RJ, Koczon-Jaremko B, Lorenzo J, Choi Y. v-ATPase VO subunit d2-deficient mice exhibit impaired osteoclast fusion and increased bone formation. Nature medicine 2006;12: 1403–1409.

[20]. Wang Y, Lebowitz D, Sun C, Thang H, Giynpas MD, Glogauer M. Identifying the relative contributions of Rac1 and Rac2 to osteoclastogenesis. J Bone Miner Res 2008;23: 260–70. [PubMed: 17922611]

[21]. Suresh Adapala Naga, Barbe MF, Tsygankov AY, Lorenzo JA, Sanjay Archana. Loss of Cbl-PI3K Interaction Enhances Osteoclast Survival due to p21-Ras Mediated PI3K Activation Independent of Cbl-b. Journal of Cellular Biochemistry 2014;1: 1–13.

[22]. Baron R, Neff L, Brown W, Courtoy PJ, Louvard D, Farquhar MG. Polarized secretion of lysosomal enzymes: co-distribution of cation-independent mannose-6-phosphate receptors and lysosomal enzymes along the osteoclast exocytic pathway. The Journal of cell biology 1988;106: 1863–1872. [PubMed: 2968345]

[23]. Teitelbaum SL. The osteoclast and its unique cytoskeleton. Ann N Y Acad Sci 2011;1240: 14–7. [PubMed: 22172034]

[24]. Karsdal MA, Martin TJ, Bollerslev J, Christiansen C, Henriksen K. Are nonresorbing osteoclasts sources of bone anabolic activity? J Bone Miner Res 2007;22: 487–94. [PubMed: 17227224]

[25]. Zhao H Membrane trafficking in osteoblasts and osteoclasts: new avenues for understanding and treating skeletal diseases. Traffic 2012;13: 1307–14. [PubMed: 22759194]

[26]. Lacombe J, Karsenty G, Ferron M. Regulation of lysosome biogenesis and functions in osteoclasts. Cell Cycle 2013;12: 2744–52. [PubMed: 23966172]

[27]. Bossard MJ, Tomaszek TA, Thompson SK, Amegadzie BY, Hanning CR, Jones C, Kurdyla JT, McNulty DE, Drake FH, Gowen M, Levy MA. Proteolytic activity of human osteoclast cathepsin K. Expression, purification, activation, and substrate identification. J Biol Chem 1996;271: 12517–12524. [PubMed: 8647860]

[28]. McQueney MS, Amegadzie BY, D'Alessio K, Hanning CR, McLaughlin MM, McNulty D, Carr SA, IJames C, Kurdyla J, Jones CS. Autocatalytic activation of human cathepsin K. J Biol Chem 1997;272: 13955–60. [PubMed: 9153258]

[29]. Holt OJ, Gallo F, Griffiths GM. Regulating secretory lysosomes. J Biochem 2006;140: 7–12. [PubMed: 16877763]

[30]. van Meel E, Boonen M, Zhao H, Oorschot V, Ross FP, Kornfeld S, Klumperman J. Disruption of the Man-6-P targeting pathway in mice impairs osteoclast secretory lysosome biogenesis. Traffic 2011;12: 912–24. [PubMed: 21466643]

[31]. Goto T, Kiyoshima T, Moroi R, Tsukuba T, Nishimura Y, Himeno M, Yamamoto K, Tanaka T. Localization of cathepsins B, D, and L in the rat osteoclast by immuno-light and - electron microscopy. Histochemistry 1994;101: 33–40. [PubMed: 8026981]

[32]. Karsdal MA, Neutzsky-Wulff AV, Dziegiel MH, Christiansen C, Henriksen K. Osteoclasts secrete non-bone derived signals that induce bone formation. Biochem Biophys Res Commun 2008;366: 483–8. [PubMed: 18068671]

[33]. Brennan T, Adapala NS, Barbe MF, Yingling V, Sanjay A. Abrogation of Cbl-PI3K interaction increases bone formation and osteoblast proliferation. Calcified tissue international 2011;89: 396–410. [PubMed: 21952831]

[34]. Lotinun S, Kiviranta R, Matsubara T, Alzate JA, Neff L, Luth A, Koskivirta I, Kleuser B, Vacher J, Vuorio E, Horne WC, Baron R. Osteoclast-specific cathepsin K deletion stimulates S1P-dependent bone formation. The Journal of clinical investigation 2013;123: 666–81. [PubMed: 23321671]

[35]. Pederson L, Ruan M, Westendorf JJ, Khosla S, Oursler MJ. Regulation of bone formation by osteoclasts involves Wnt/BMP signaling and the chemokine sphingosine-1-phosphate. Proc Natl Acad Sci U S A 2008;105: 20764–9. [PubMed: 19075223]

[36]. Drake FH, Dodds RA, James IE, Connor JR, Debouck C, Richardson S, Lee-Rykaczewski E, Coleman L, Rieman D, Barthlow R, Hastings G, Gowen M. Cathepsin K, but not cathepsins B, L, or S, is abundantly expressed in human osteoclasts. J Biol Chem 1996;271: 12511–6. [PubMed: 8647859]

[37]. Everts V, Aronson DC, Beertsen W. Phagocytosis of bone collagen by osteoclasts in two cases of pycnodysostosis. Calcif Tissue Int 1985;37: 25–31. [PubMed: 3922593]

[38]. Everts V, Korper W, Hoeben KA, Jansen ID, Bromme D, Cleutjens KB, Heeneman S, Peters C, Reinheckel T, Saftig P, Beertsen W. Osteoclastic bone degradation and the role of different cysteine proteinases and matrix metalloproteinases: differences between calvaria and long bone. J Bone Miner Res 2006;21: 1399–408. [PubMed: 16939398]

[39]. Saftig P, Hunziker E, Wehmeyer O, Jones S, Boyde A, Rommerskirch W, Moritz JD, Schu P, von Figura K. Impaired osteoclastic bone resorption leads to osteopetrosis in cathepsin-K-deficient mice. Proc Natl Acad Sci U S A 1998;95: 13453–13458. [PubMed: 9811821]

[40]. Gelb BD, Shi G-P, Chapman HA, Desnick RJ. Pycnodysostosis, a lysosomal disease caused by cathepsin K deficiency. Science 1996;273: 1236–1238. [PubMed: 8703060]

[41]. Li CY, Jepsen KJ, Majeska RJ, Zhang J, Ni R, Gelb BD, Schaffler MB. Mice lacking cathepsin K maintain bone remodeling but develop bone fragility despite high bone mass. J Bone Miner Res 2006;21: 865–75. [PubMed: 16753017]

[42]. Cremasco V, Decker CE, Stumpo D, Blackshear PJ, Nakayama KI, Nakayama K, Lupu TS, Graham DB, Novack DV, Faccio R. Protein kinase C-delta deficiency perturbs bone homeostasis by selective uncoupling of cathepsin K secretion and ruffled border formation in osteoclasts. J Bone Miner Res 2012;27: 2452–63. [PubMed: 22806935]

[43]. Hou JC, Pessin JE. Ins (endocytosis) and outs (exocytosis) of GLUT4 trafficking. Curr Opin Cell Biol 2007;19: 466–73. [PubMed: 17644329]

[44]. Chen S, Murphy J, Toth R, Campbell DG, Morrice NA, Mackintosh C. Complementary regulation of TBC1D1 and AS160 by growth factors, insulin and AMPK activators. Biochem J 2008;409: 449–59. [PubMed: 17995453]

[45]. Ren W, Cheema S, Du K. The association of ClipR-59 protein with AS160 modulates AS160 protein phosphorylation and adipocyte Glut4 protein membrane translocation. J Biol Chem 2012;287: 26890–900. [PubMed: 22689584]

[46]. Jackson TR, Kearns BG, Theibert AB. Cytohesins and centaurins: mediators of PI 3-kinase-regulated Arf signaling. Trends Biochem Sci 2000;25: 489–95. [PubMed: 11050434]

[47]. Soundararajan M, Yang X, Elkins JM, Sobott F, Doyle DA. The centaurin gamma-1 GTPase-like domain functions as an NTPase. Biochem J 2007;401: 679–88. [PubMed: 17037982]

[48]. DeSelm CJ, Miller BC, Zou W, Beatty WL, van Meel E, Takahata Y, Klumperman J, Tooze SA, Teitelbaum SL, Virgin HW. Autophagy proteins regulate the secretory component of osteoclastic bone resorption. Dev Cell 2011;21: 966–74. [PubMed: 22055344]

[49]. Sandilands E, Serrels B, McEwan DG, Morton JP, Macagno JP, McLeod K, Stevens C, Brunton VG, Langdon WY, Vidal M, Sansom OJ, Dikic I, Wilkinson S, Frame MC. Autophagic targeting of Src promotes cancer cell survival following reduced FAK signalling. Nat Cell Biol 2011;14: 51–60. [PubMed: 22138575]

[50]. Segovia-Silvestre T, Neutzsky-Wulff AV, Sorensen MG, Christiansen C, Bollerslev J, Karsdal MA, Henriksen K. Advances in osteoclast biology resulting from the study of osteopetrotic mutations. Hum Genet 2009;124: 561–77. [PubMed: 18987890]

[51]. Pennypacker B, Shea M, Liu Q, Masarachia P, Saftig P, Rodan S, Rodan G, Kimmel D. Bone density, strength, and formation in adult cathepsin K (−/−) mice. Bone 2009;44: 199–207. [PubMed: 18845279]

[52]. Martin TJ, Sims NA. Osteoclast-derived activity in the coupling of bone formation to resorption. Trends in molecular medicine 2005;11: 76–81. [PubMed: 15694870]

[53]. Weilbaecher KN, Guise TA, McCauley LK. Cancer to bone: a fatal attraction. Nat Rev Cancer 2011;11: 411–25. [PubMed: 21593787]

[54]. Brubaker KD, Vessella RL, True LD, Thomas R, Corey E. Cathepsin K mRNA and protein expression in prostate cancer progression. J Bone Miner Res 2003;18: 222–30. [PubMed: 12568399]

[55]. Littlewood-Evans AJ, Bilbe G, Bowler WB, Farley D, Wlodarski B, Kokubo T, Inaoka T, Sloane J, Evans DB, Gallagher JA. The osteoclast-associated protease cathepsin K is expressed in human breast carcinoma. Cancer Res 1997;57: 5386–90. [PubMed: 9393764]

[56]. Buonamici S, Williams J, Morrissey M, Wang A, Guo R, Vattay A, Hsiao K, Yuan J, Green J, Ospina B, Yu Q, Ostrom L, Fordjour P, Anderson DL, Monahan JE, Kelleher JF, Peukert S, Pan S, Wu X, Maira SM, Garcia-Echeverria C, Briggs KJ, Watkins DN, Yao YM, Lengauer C, Warmuth M, Sellers WR, Dorsch M. Interfering with resistance to smoothened antagonists by inhibition of the PI3K pathway in medulloblastoma. Sci Transl Med 2010;2: 51ra70.

[57]. Folkes AJ, Ahmadi K, Alderton WK, Alix S, Baker SJ, Box G, Chuckowree IS, Clarke PA, Depledge P, Eccles SA, Friedman LS, Hayes A, Hancox TC, Kugendradas A, Lensun L, Moore P, Olivero AG, Pang J, Patel S, Pergl-Wilson GH, Raynaud FI, Robson A, Saghir N, Salphati L, Sohal S, Ultsch MH, Valenti M, Wallweber HJ, Wan NC, Wiesmann C, Workman P, Zhyvoloup A, Zvelebil MJ, Shuttleworth SJ. The identification of 2-(1H-indazol-4-yl)-6-(4-methanesulfonyl-piperazin-1-ylmethyl)-4-morpholin-4-yl-t hieno[3,2-d]pyrimidine (GDC-0941) as a potent, selective, orally bioavailable inhibitor of class I PI3 kinase for the treatment of cancer. J Med Chem 2008;51: 5522–32. [PubMed: 18754654]

[58]. Maira SM, Stauffer F, Brueggen J, Furet P, Schnell C, Fritsch C, Brachmann S, Chene P, De Pover A, Schoemaker K, Fabbro D, Gabriel D, Simonen M, Murphy L, Finan P, Sellers W, Garcia-Echeverria C. Identification and characterization of NVP-BEZ235, a new orally available dual phosphatidylinositol 3-kinase/mammalian target of rapamycin inhibitor with potent in vivo antitumor activity. Mol Cancer Ther 2008;7: 1851–63. [PubMed: 18606717]

Highlights

1. Cbl-PI3K interaction regulates Cathepsin K secretion, but secretion of Cathepsin D is normal.
2. Absence of Cbl-PI3K interaction reduces numbers of LAMP2 positive secretory lysosomes.
3. Dysfunctional osteoclasts derived from YF mutant mice secrete factor that promote osteogenesis.

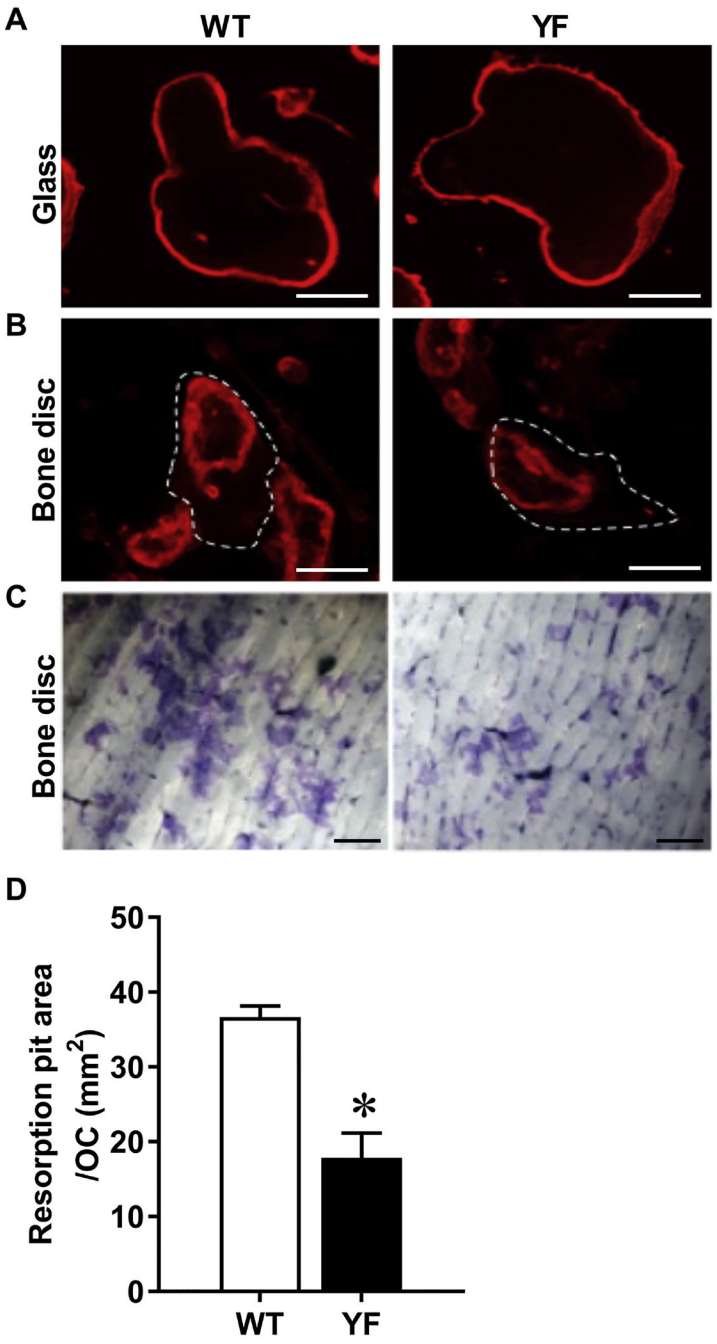

Figure 1.

Actin organization and sealing zone formation are not altered, but bone-resorbing activity is decreased in YF osteoclasts. BMMs were cultured in collagen gel with M-CSF and RANKL for 6 days. Mature osteoclasts were released by treating cultures with 0.1% Collagenase, and cells were plated on glass cover slips (A) or bovine bone discs (B and C). Cells were stained with rhodamine-phalloidin to visualize actin ring (A) and sealing zone (B) formation (orange). Dotted lines indicate boundaries of osteoclasts. (C) Bone discs were stained with toluidine blue to visualize pit formation. (D) Stained area was quantified and normalized for

the numbers of osteoclasts. Values are mean ± SD, n=9, * Significantly different between WT and YF, $p < 0.05$. Scale bars represent 100 μM and 50 μM for (A) and (B), respectively.

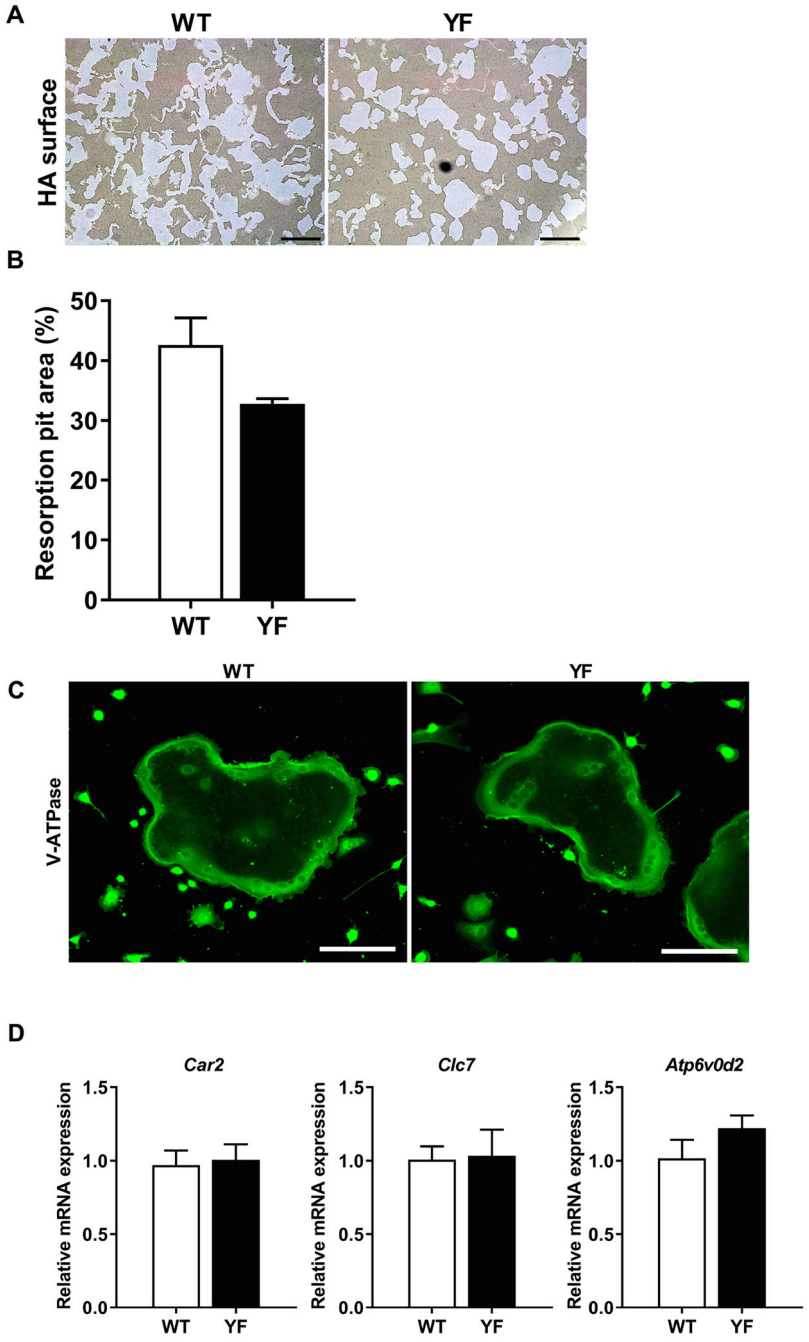

Figure 2.

YF osteoclasts can resorb HA-coated surface. (A) Mature osteoclasts were plated on HA-coated surface and resorbed area was visualized. (B) Percentage of total resorbed area is indicated. (C) Cells cultured on coverslips were immunostained for v-ATPase (E subunit, green) using an antibody that was a gift from Dr. Beth Lee, OSU. Similar distribution of v-ATPase was observed for both genotypes. (D) mRNA levels of *Car2, Clc7,* and *Atp6v0d2* were analyzed by qRT-PCR and were normalized my mRNA levels of *Gapdh.* Values are mean ± SD, n=5. Scale bar represents 100 μM for (A) and (C).

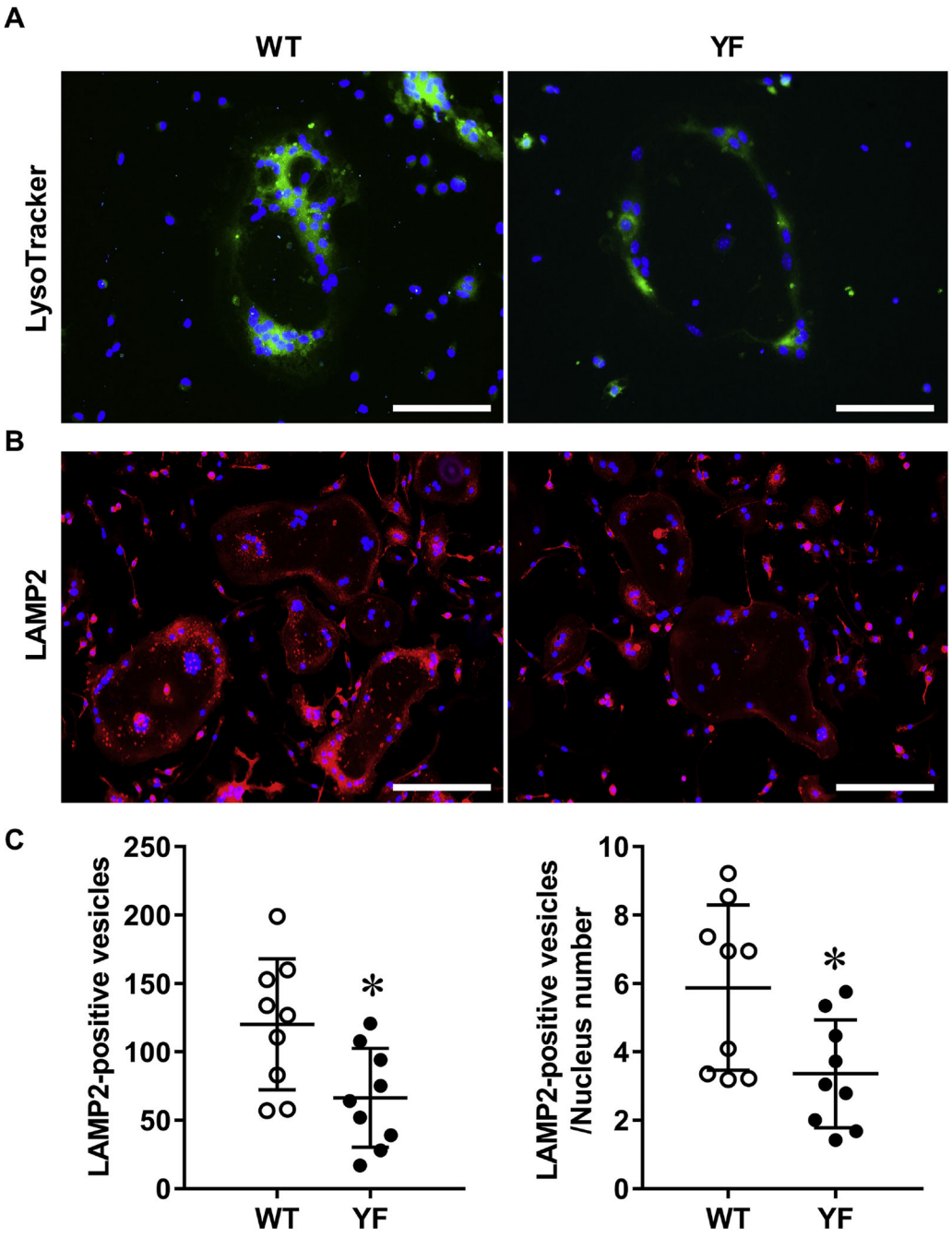

Figure 3.

The number of LAMP2-positive vesicles is decreased in YF osteoclasts. Mature osteoclasts seeded on glass cover slips were fixed and stained with LysoTracker® fluorescent dye (green) (A) or anti-LAMP2 antibodies (red) (B) with DAPI to visualize (blue). (C) Numbers of LAMP2-positive lysosomes. To count LAMP2-positive lysosomes 8 osteoclasts were observed (left) and the lysosome number was normalized to number of nuclei/osteoclast (right). Experiment was performed three times, each time using a different cohort of WT and YF mice. A representative experiment is shown. Values are mean ± SD, * Significance

different between WT and YF, $p < 0.05$. Scale bars represent 100 μM and 200 μM for (A) and (B) respectively.

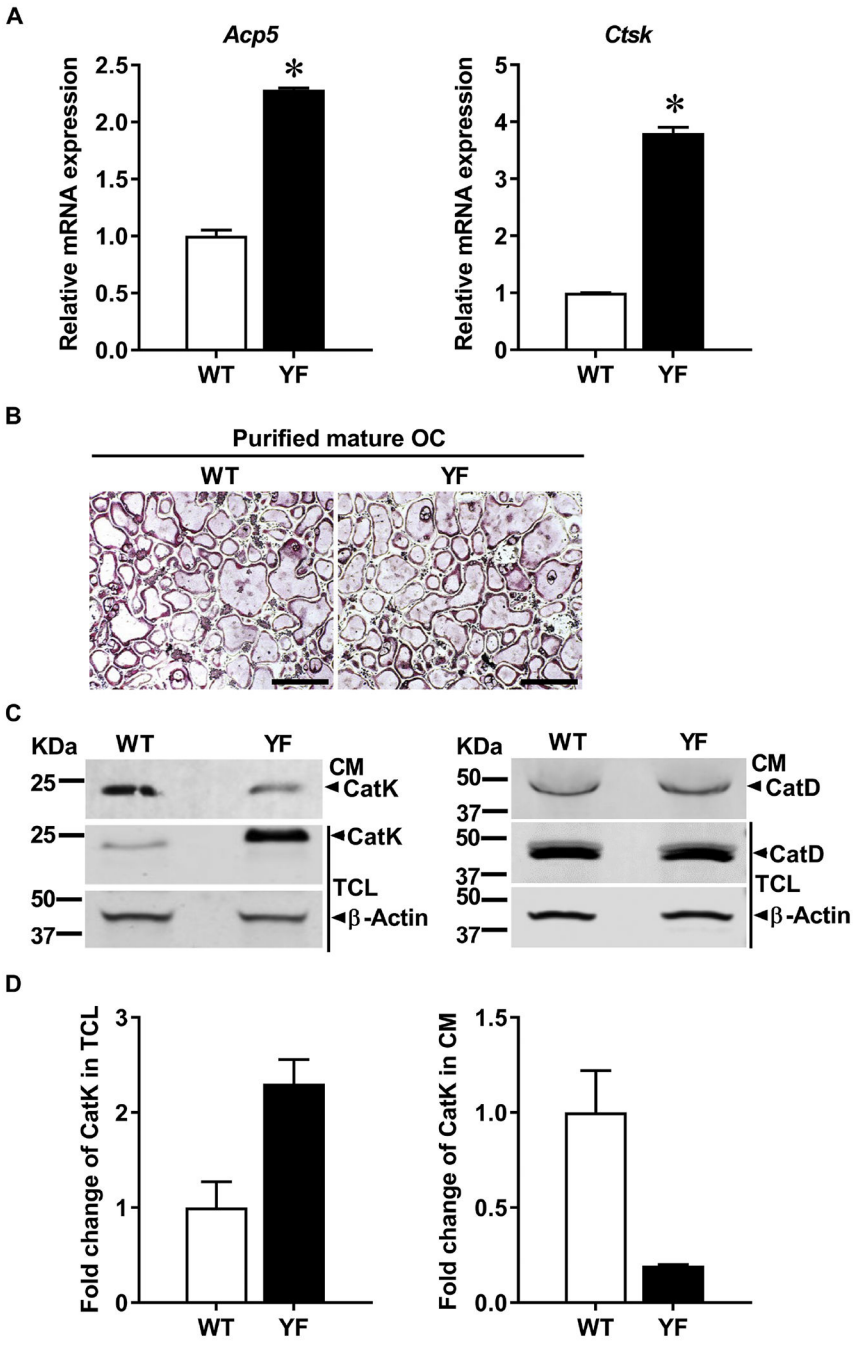

Figure 4.

Cathepsin K secretion is perturbed in YF osteoclasts. (A) mRNA expression of *Acp5* and *Ctsk* was examined by qRT-PCR and normalized by mRNA level of *Gapdh.* Values are mean ± SD, n=3, *Significant difference between WT and YF, $p < 0.05$. (B) Equal numbers of purified mature osteoclasts (OC) seeded on tissue culture plastic were stained for TRAP. Scale bar 200 μM (C) Equal numbers of mature osteoclasts seeded in 24-well plates were cultured in medium containing 10% FBS overnight. Total cell lysate (TCL) (50 μg) and conditioned media (CM) (25 μ́) were electrophoresed on 10 or 12% SDS-PAGE gels.

Western blots were probed with anti-Cathepsin K (CatK) (left) and anti-Cathepsin D (CatD) (right) antibodies. Only the mature CatK form is shown. Blots were stripped and reprobed with anti-β-Actin antibodies to verify equal loading of TCL. (D) Signal intensity of CatK protein bands in technical duplicates was quantified using LI-COR (Odyssey) system. Experiment was performed three times, each time using a different cohort of WT and YF mice. A representative experiment is shown.

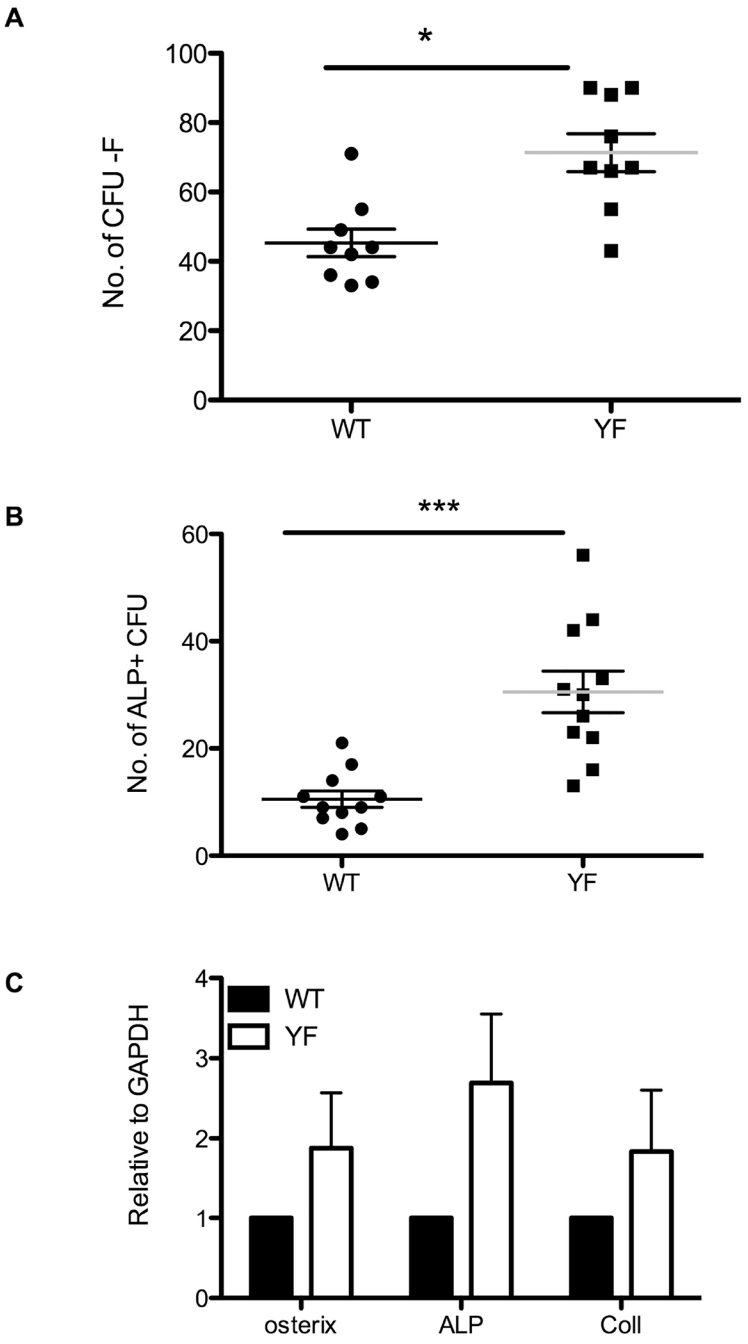

Figure 5.

Conditioned media from YF osteoclasts induces osteogenesis. WT calvarial-derived osteoblasts (OB) (10^5 cells/well) in 6-well plates were grown in triplicates in conditioned media (CM) derived from mature osteoclast cultures. After 7 days, colonies were fixed and stained with toluidine blue to stain CFU fibroblasts (A) or with ALP to stain for CFU-OB (B). Groups of 20 or more cells were counted as a colony. (C) Colonies were harvested after 7 days and expression of osteogenic markers was performed by qRT-PCR and normalized by

mRNA level of *Gapdh*. Values are mean ± SD, and plotted as relative expression to WT. A representation of 2 experiments is shown.

Table 1.

Primers used for real-time PCR

Gene	Forward primer	Reverse primer
Atp6v0d2	CAATGAAGCGTCACCTCTGA	TCAGCTATTGAACGCTGGTG
Ctsk	CAGCTTCCCCAAGATGTGAT	AAAAATGCCCTGTTGTGTCC
CA2	CAAGCACAACGGACCAGA	ATGAGCAGAGGCTGTAGG
Clcn7	GACTGGCTGTGGGAA	TCTCGCTTGAGTGATGTTGAC C
Acp	GCAGCTCCCTAGAAGATGGATT	ATTTGTAGGCCCAGCAGCAC
Mtif	TTGATGGATCCGGCCTTGCAAATG	TATGTTGGGAAGGTTGGCTGGACA
Tfeb	GTCATTGACAACATTATGCGCC	GCGTGTTAGGCATCTTGCATCT
Tfe3	CCAAGCTGGCTTCCCAGGCTCTCAC	GTTAATGTTGAATCGCCTGCGTCG
Wnt10B	AGGCTTCTCCTTCCGTTCAGTTGT	ATTCCCACCCTTCCTGCTGAAGAA
PDGF-BB	GGGATCCCATTCCTGAGGAAC	CGGTCCAGGTGAGAAAGATTG
Sema4D	TCTTTGCTGACGTGATCCAG	CAGATCAGCCTGGCCTTTAG
Sphk1	TGAGGTGGTGAATGGGCTAATGGA	AACAGCAGTGTGCAGTTGATGAGC
Sphk2	TGGGCTGTCCTTCAACCTCATACA	AGTGACAATGCCTTCCCACTCACT
Bmp6	AGAAGGGCACTCTTTCAGGTTCCA	TCACACCACCGAGAGTCAACACAA
Osterix	GATGGCGTCCTCTCTGCTTG	GCCATAGTGAGCTTCTTCCTCAA
ALP	GGAGATGGTATGGGCGTCTC	CTGGCCCTTAAGGATTCGGG
Col1a1	CGATGGATTCCCGTTCGAGT	ACATTAGGCGCAGGAAGGTC
Gapdh	AGGTCGGTGTGAACGGATTTG	TGTAGACCATGTAGTTGAGGTCA

Table 2:

Expression analysis of osteogenic factors generated by WT and YF osteoclasts

	WT	YF
PDFG-BB	1.08 ± 0.150	0.972 ± 0.414
BMP6	1.06 ± 0.138	1.602 ± 0.039
Sema4 D	1.017 ± 0.216	1.220 ± 0.174
Sphk-1	1. 27 ± 0.016	0.945 ± 0.204
Sphk-2	0.956 ± 0.03	0.987 ± 0.131
Wnt10b	1.00 ± 0.012	0.823 ± 0.041

WT calvarial osteoprogenitors in triplicates were treated with conditioned media-derived from WT and YF mice for seven days. mRNA expression was analyzed by qRT-PCR and were normalized by mRNA levels of *Gapdh.* Values are mean ± SD, n=3.